Enabling City-scale Multi-energy Optimal Dispatch with Energy Hubs

Mads R. Almassalkhi and Anna Towle

School of Engineering

University of Vermont

Burlington, Vermont, USA

{malmassa, atowle}@uvm.edu

Abstract—This paper further extends the class of energy hubs that can be modeled with a concise system description and in a computationally efficient optimization framework to permit rapid analysis of multi-energy systems. The new hub models are then embedded in the multi-energy system analysis tool Hubert and solves the multi-period optimal dispatch (MPOD) problem for a broad class of energy hub systems. Specifically, this paper presents recent improvements developed for Hubert, including the use of piece-wise linear modeling to capture nonlinear converter efficiencies, limits on hub component outputs to reflect physical limits of converters, and hub emission limits. These developments enable appropriate modeling of multi-energy micro-grids and cities and are illustrated with a multi-energy model of The University of Vermont's campus under different capital planning scenarios and modeling assumptions. Interestingly, the shortcomings of using a traditional constant-efficiency hub converter model are illustrated with an energy storage sizing application for multi-energy systems. It is shown that the traditional hub models can significantly undersize energy storage as compared to the more accurate piece-wise linear energy hub formulation.

Index Terms— coupled energy infrastructures, energy hubs, piece-wise linear modeling, multi-period optimal dispatch, optimization, energy storage.

I. Introduction and Motivation

The emphasis on integrating renewables, coordination of building loads, the marked change in generator fleet make-up, and emissions have placed a renewed focus on the reliability and optimality of energy supply systems [1]. Such systems involve interconnections between the electrical networks and various energy carriers, such as natural gas, water, heating, and cooling. For example, electricity produced from thermal generators involves large amounts of water and, in Australia, a drought negatively affected the electric production capabilities [2]. Similarly, extreme winter temperatures in Northeastern US constrained natural gas pipeline networks and resulted in lower-than-expected electrical operating reserves by the ISO [3]. At the scale of cities and large manufacturing facilities (e.g., "Virtual Power Plants"), the demand takes on a multi-energy form: electricity, heating, and cooling and requires multiple applications of lossy energy conversion and storage

processes [4]. Such interconnected energy systems motivate the concept of the energy hub [5]. Energy hub concepts provide a modeling framework for extending beyond specific energy carrier combinations and allowing analysis and optimization of an arbitrary array of energy systems. Modeling the coupled systems may reveal minimum cost solutions, and also vulnerabilities, that are not apparent when each system is treated separately.

Related Works: The formal combination of multi-energy carriers with processes was performed under the nonlinear modeling framework of the "energy hub" [6], [7]. The energy hub framework enabled innovative studies in: distributed predictive control of energy hub systems, impact of hybrid-electric transportation, integration of energy storage, and multi-energy analysis of buildings [8]–[10]. An equivalent, but linear formulation of energy hubs was developed to create a modeling and optimization tool for general energy hub systems: Hubert, which is detailed in [11] and utilized herein. Hubert's original constant efficiency and linear power-flow assumptions permitted investigations into large-scale multi-period optimal dispatch of energy hub networks and the role of energy storage in mitigating multi-energy cascade failures [12], [13].

More recently, the energy hub formulation has gained traction in modeling of residential and industrial multi-energy systems (e.g., heating, cooling, electric) [14]–[18]. However, when the focus of analysis is on dispatching converters in individual energy hubs rather than across large multi-carrier networks, it is important to validate assumptions made on the efficiency of energy processes. For example, in the case of material inflow and outflow rates, lossless flows are natural [19]. However, heating and cooling processes in an industrial setting (e.g., steam boilers and vapor-compression chillers) rarely exhibit constant efficiency over any meaningful range of operation [20]. In fact, the relationship between energy input and output is often not even convex (i.e., the efficiency increases and decreases across the operating range). As a result, nominal or averaged efficiency values can lead to poor representative models for energy conversion processes as efficiency tends to decrease rapidly at part-load. In addition, constant efficiency results in hub dispatches that under-estimate required fuel costs and resulting emissions.

Few energy hub formulations and studies consider the nonlinearity of hub converters. However, one particularly

interesting application of a detailed building-level energy hub can be found in [10], where individual conversion-processes are available in one energy hub and modeled with highly nonlinear part-load efficiency curves. The resulting model represents a nonlinear programming formulation for the energy hub that is solved to a local optimum and for which few numerically robust solvers exist. In addition, no energy storage is considered, whose temporal coupling of decision variables further complicates the formulation. For a detailed discussion on multi-energy systems (MES) and energy hubs, see [1].

Contributions: This paper extends the modeling of energy hubs to a more general class with nonlinear conversion processes and illustrates these techniques with the energy hub optimization tool "Hubert" to enable modeling of macro-grid MES (e.g., transmission) and micro-grid MES (e.g., campus or city). Specifically, the paper develops a mixed-integer piecewise linear programming formulation of a general energy hub system that captures nonlinear energy conversion processes, energy storage, and hub emission limits. This paper overcomes the numerical difficulties associated with the nonlinear energy hub model in [10] by explicitly considering a piece-wise linear approximation of part-load input-output curves of energy hub converters to capture the variable part-load efficiency. This PWL approximation is then implemented within Hubert to permit rapid analysis of general MES. The flexible Hubert modeling framework is illustrated with a case study on university campus MES and permits rapid analysis of different investment scenarios for energy hub components (e.g., storage and combined heat-and-power facilities). Finally, the proposed piece-wise linear energy hub formulation is employed to highlight the shortcomings of the traditional constant-efficiency energy hub models with an energy-storage sizing problem for MES.

Section II details the development of the piece-wise linear energy hub modeling framework. In Section III, we outline the automatic modeling tool Hubert while Section IV employs Hubert to model an actual university campus. Finally, Section V concludes the paper with discussion and future directions.

II. Modeling the Energy Hub

Most general energy hubs can be constructed from interconnections of five simple building blocks: input energy sources, input energy storage, energy converters, output energy storage, and output energy sinks. These five building blocks are illustrated in Figure 1. In describing the flow of energy from hub input to hub output, there is a need to consider the flow between each of the five blocks of the hub.

A. Linear Hub Model

Let $h \in \mathscr{H}$ be a hub from the set of available hubs, where h has input sources $i \in \{1, 2, \ldots, N_{in}\}$ and output sources $n \in \{1, 2, \ldots, N_{out}\}$.

The main mathematical symbols used in this paper to model the energy hub h are classified below for quick reference.

P_i - hub energy flow input i.
Q_i^{in} - hub input-side energy storage flow from input i.
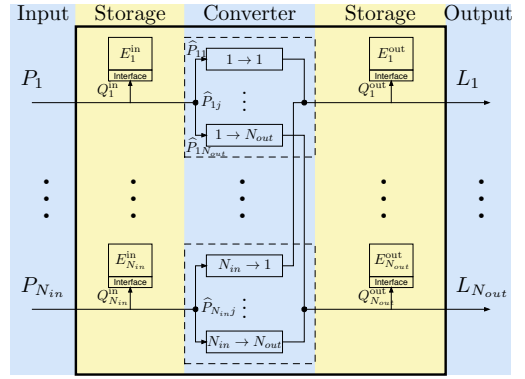E_i^{in} - hub input-side energy storage state-of-charge at input i.

Figure 1: A complete energy hub model illustrating all possible energy-conversion paths and the five major hub building blocks: input sources, input storage, converters, output storage, and output sinks.

$\eta_{\text{c/d},i}^{\text{in}}$ - hub storage interface charge (c) / discharge (d) efficiencies at input i.
$\widehat{P}_{ij}$ - hub dispatch energy flow from input i directed to converter j.
C_{ijn} - efficiency of converting energy input i into output type n through converter j.
Q_n^{out} - hub output-side energy storage flow to output n.
$\eta_{\text{c/d},n}^{\text{out}}$ - hub storage interface charge (c) / discharge (d) efficiencies at output n.
E_n^{out} - hub output-side energy storage SOC at output n.
L_n - hub energy flow output n.
$z_{i/n}^{\text{in/out}}$ - binary hub storage operational status: charging ($= 1$) or discharging ($= 0$).

Within the proposed energy hub modeling framework, energy conversion ($\widehat{P}$) and energy storage utilization processes (Q) can be directly controlled (i.e., other variables are dependent). Under the assumption of constant conversion and storage efficiencies, previous work has shown that the energy hub with storage can be modeled with a mixed-integer linear formulation by using dispatch flows $\widehat{P}_{ij}$ [12]. The binary integers arise because storage processes may not charge and discharge simultaneously. Summarizing the previous results, the energy flow from input i to output n is illustrated in Fig. 2 and described by the following relations:

$$P_i = Q_i^{in} + \sum_{j=1}^{K_i} \widehat{P}_{ij} \qquad (1)$$

$$\sum_i \sum_{j \in \mathcal{D}(i,n)} C_{ijn} \widehat{P}_{ij} = Q_n^{out} + L_n \qquad (2)$$

where $\widehat{P}_{ij} \geq 0$ and $K_i \leq N_{out}$ is the number of dispatch flows from input i and $\mathcal{D}(i,n)$ is the set of dispatch flows from input i that can be converted to output n, and $|\mathcal{D}(i,n)| \leq K_i$.

With regard to input and output energy storage devices, one must consider multiple time periods since, for energy source p, the state-of-charge (SOC) at time $k + 1$ (over a time interval T_s), depends on the SOC and charge/discharge rate in the
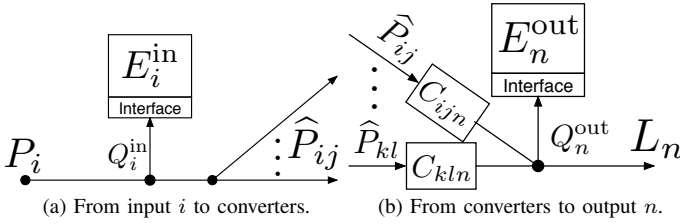
Figure 2: Energy hub model based on dispatch flows $\widehat{P}_{ij}$.

(a) From input i to converters. (b) From converters to output n.

Figure 3: Typical steam boiler input-output curve with linear and 4-segment PWL approximations.

previous time step k. To simplify notation, input and output storage denotations, $(.)^{\text{in/out}}$, are omitted here.

$$E_p[k+1] = E_p[k] + T_s \eta_{c,p} Q_{c,p}[k] + \frac{T_s}{\eta_{d,p}} Q_{d,p}[k] \quad (3)$$

$$Q_p[k] = Q_{c,p}[k] + Q_{d,p}[k] \quad (4)$$

$$(z_p[k]-1)\underline{Q}_p \leq Q_{d,p}[k] \leq 0 \quad (5)$$

$$0 \leq Q_{c,p}[k] \leq z_p[k]\,\overline{Q}_p \quad (6)$$

$$0 \leq E_p[k] \leq \overline{E}_p \quad (7)$$

where $z_p[k] \in \{0,1\}$, $\overline{Q}_p$ and $\underline{Q}_p$ are constant power ratings of device p, and $\overline{E}_p$ is the energy rating of device p. Thus, when $z_p[k] \equiv 0$, storage device p is in discharging mode at time k (as $Q_{c,p}[k] \equiv 0$), while $z_p[k] \equiv 1$ implies p is in charging mode (with $Q_{p,dis}[k] \equiv 0$) at time k.

1) Matrix notation for energy hub model: Consider discrete time-steps k. The linear relations between inputs and outputs can be written in a compact matrix form:

$$\mathbf{P}_h[k] = \mathbf{S}_h^{in}\mathbf{Q}_h^{in}[k] + \mathbf{F}_h\widehat{\mathbf{P}}_h[k] \quad (8)$$

$$\mathbf{E}_h[k+1] = \mathbf{E}_h[k] + \mathbf{N}_{c,h}\mathbf{Q}_{c,h}[k] + \mathbf{N}_{d,h}\mathbf{Q}_{d,h}[k] \quad (9)$$

$$\mathbf{Q}_h[k] = \mathbf{Q}_{c,h}[k] + \mathbf{Q}_{d,h}[k] \quad (10)$$

$$\mathbf{Q}_{c,h}[k] \leq \mathbf{z}_h[k]\overline{\mathbf{Q}}_h \quad (11)$$

$$(\mathbf{1}-\mathbf{z}_h[k])\underline{\mathbf{Q}}_h \leq \mathbf{Q}_{d,h}[k] \quad (12)$$

$$\mathbf{L}_h[k] = \mathbf{C}_h\widehat{\mathbf{P}}_h[k] + \mathbf{S}_h^{out}\mathbf{Q}_h^{out}[k] \quad (13)$$

for all $h \in \mathcal{H}$ where $\mathbf{S}_h^{in}$ is the *input storage coupling matrix*, $\mathbf{F}_h$ is the *dispatch flow matrix*, $\mathbf{C}_h$ is the *converter coupling matrix* and $\mathbf{S}_h^{out}$ is the *output storage coupling matrix*. Note that $\mathbf{N}_{c,h} = \mathrm{diag}(\eta_{c,1},\ldots,\eta_{c,N})$ and $\mathbf{N}_{d,h} = \mathrm{diag}(1/\eta_{d,1},\ldots,1/\eta_{d,N})$ are diagonal matrices of charging and discharging efficiencies, respectively, and are independent of the potentially complex internal hub structure (input-output connections)

Furthermore, since each hub h is completely described by its local matrices $\mathbf{S}_h^{in}$, $\mathbf{F}_h$, $\mathbf{C}_h$, and $\mathbf{S}_h^{out}$, each hub is decoupled and one can describe the entire set of hubs $\mathcal{H}$ by constructing block-matrices from the h-specific matrices. For example, the converter coupling matrix for the entire set $\mathcal{H}$ is defined by $\mathbf{C} = \mathrm{diag}\{\mathbf{C}_1,\ldots,\mathbf{C}_{|\mathcal{H}|}\}$.

Thus, the above presents a linear formulation of a general energy hub. The linear model is amenable to straightforward (mixed-integer) linear optimization and guarantees that optimal solutions are globally optimal. In addition, the mixed-integer formulation of the energy storage model can be relaxed depending on 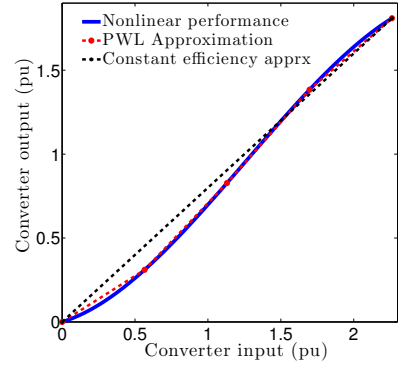the optimization problem and, therefore, the linear hub formulation above enables a strictly linear and continuous hub model. Having a linear model permits large-scale simulations of multi-energy systems, which is explored in [13], [21].

Remark 1. Notice that linearity rests on the assumption that the coupling matrices are constant. Specifically, consider the converter coupling matrix $\mathbf{C}_h$ (i.e., converter efficiencies). As discussed in detail in [20], the efficiency of most energy conversion processes depends on the part-load rating of device. The nonlinear efficiency curve of a typical natural-gas-to-steam boiler has maximum efficiency occur at around 90-95% rated capacity. Since

$$\text{efficiency} = \text{energy output} / \text{energy input}$$
$$\Rightarrow \text{ energy output} = \text{efficiency} \times \text{energy input},$$

the relationship between converter input and output is nonlinear, but monotonic as illustrated in Fig. 3. As such, we need to investigate an input-output formulation that permits tractable implementation of these nonlinear energy hub converters.

B. Piece-wise Linear Converters

Consider a single-input single-output energy hub with no energy storage but a nonlinear converter. The hub equations are then straightforward:

$$P = \widehat{P} \quad \text{and} \quad L = f_c(\widehat{P}) \quad (14)$$

Where f_c is the nonlinear (input-output) performance curve of converter c, see Fig. 3. Our emphasis is then on the converter input-output relation in Eq. (14). Now, select a set of $S+1$ salient input values and evaluate f_c at those points (e.g., $f_c^s = f_c(\widehat{P}^s)$):

$$\{\widehat{P}^1\widehat{P}^2,\ldots,\widehat{P}^{S+1}\} \text{ and } \{f_c^1, f_c^2, \ldots, f_c^{S+1}\}.$$

Segment s is then the linear segment between input-output pairs $(\widehat{P}^s, f_c^s)$ and $(\widehat{P}^{s+1}, f_c^{s+1})$ with α_s defined as the slope of segment s. Since additional input energy always begets increased output energy (i.e., f_c is monotonic), $\alpha_s > 0, \forall s$.

Now, the piece-wise linear approximation of (14) can be defined as:

$$L = f_c(\widehat{P}) \approx \text{PWL}[f_c(\widehat{P})] = \sum_{s=1}^{S} \alpha_s \Delta \widehat{P}^s \qquad (15)$$

where a new dispatch flow variable, $\Delta \widehat{P}^s$, is associated with each PWL segment s and

$$\widehat{P} = \sum_{s=1}^{S} \Delta \widehat{P}^s, \quad \Delta \widehat{P}^s \in [0, \widehat{P}^{s+1} - \widehat{P}^s] =: [0, \Delta_P^s] \quad (16)$$

However, since the efficiency curve need not be monotonic, the rate at which f_c increases is not monotonic, which implies that f_c is not a convex function. This condition requires additional adjacency conditions[1] to be enforced among the $S > 1$ segment variables. Define binary adjacency variables $y_m \in \{0, 1\}$ for $m = 1, 2, \ldots, 2(S-2)$, then we have the following S segment constraints:

For $s = 1$: $\qquad y_s \Delta_P^s \leq \Delta \widehat{P}^s \leq \Delta_P^s \qquad (17)$

For $2 \leq s \leq S-1$: $\quad y_{2s-2}\Delta_P^s \leq \Delta \widehat{P}^s \leq y_{2s-1}\Delta_P^s \quad (18)$

For $s = S$: $\qquad 0 \leq \Delta \widehat{P}^s \leq y_{2s-2}\Delta_P^s \qquad (19)$

where the $2(S-1)$ adjacency variables y_m are inter-related via the following $2S - 3$ adjacency constraints:

For $m = 1$: $\begin{cases} y_{m+1} \leq y_m \\ y_{m+2} \leq y_m \end{cases}$ $\qquad (20)$

For $m = 2, 4, 6, \ldots, 2(S-3)$: $\begin{cases} y_{m+2} \leq y_m \\ y_{m+3} \leq y_m \end{cases}$ $\quad (21)$

For $m = 2(S-2)$: $\quad y_{m+2} \leq y_m. \qquad (22)$

Of course, if $S = 1$, there is no need for adjacency conditions or variables y_m and for $S = 2$ only constraints (20) and (22) are necessary.

1) PWL Example: Consider a PWL converter approximated with $S = 4$ segments as in Fig. 3, then for each time-step the following 10 variables are added:

$$\Delta \widehat{P}^1, \Delta \widehat{P}^2, \Delta \widehat{P}^3, \Delta \widehat{P}^4, y_1, y_2, y_3, y_4, y_5, y_6$$

with the following 11 constraints:

$$\begin{aligned} y_1 \Delta_P^1 &\leq \Delta \widehat{P}^1 \leq \Delta_P^1 & y_2 &\leq y_1 \\ y_2 \Delta_P^2 &\leq \Delta \widehat{P}^2 \leq y_3 \Delta_P^2 & y_3 &\leq y_1 \\ y_4 \Delta_P^3 &\leq \Delta \widehat{P}^3 \leq y_5 \Delta_P^3 & y_4 &\leq y_2 \\ 0 &\leq \Delta \widehat{P}^4 \leq y_6 \Delta_P^4 & y_5 &\leq y_2 \\ & & y_6 &\leq y_4 \end{aligned}$$

To illustrate the adjacency condition, suppose that $\Delta \widehat{P}^3 > 0 \Rightarrow y_5 = 1 \Rightarrow y_2 = 1 \Rightarrow y_3 = 1 \Rightarrow \Delta \widehat{P}^2 = \Delta_P^2$ and $y_1 = 1 \Rightarrow \Delta \widehat{P}^1 = \Delta_P^1$. Clearly, this satisfies adjacency condition.

The PWL formulation with $S = 4$ accurately captures the nonlinear converter performance as shown in Fig. 3 and, therefore, the underlying nonlinear efficiency at part-load operation. The constant efficiency can greatly underestimate

[1]Adjacency implies that if $\Delta \widehat{P}^s > 0$, then $\Delta \widehat{P}^l \equiv \Delta_P^l \; \forall l < s$

the converter input (e.g., natural gas) needed to produce a given output (e.g., steam) at part-load operating conditions.

Remark 2. The PWL approximation of a nonlinear energy hub converter with $S \geq 3$ segments adds S continuous and $2(S-1)$ binary variables and $2(S-1) + (2S-3) \times 2 = 4S - 5$ constraints (i.e., simple bound are not constraints in this context) to the formulation and scales linearly with the number of converters and time-steps.

2) Converter Limits: Another improvement in the energy hub converter model is the addition of converter output limits to represent finite capacity of converters (e.g., maximum boiler output capacity) and also is the basis on which to effectively dispatch (i.e. stage) multiple converters:

$$\sum_{s=1}^{S} \alpha_s \Delta \widehat{P}^s[k] \leq \overline{L}. \qquad (23)$$

One can now replace the constant-efficiency model from (13) with the PWL approximation described above (and generalized to multi-input/multi-output energy hubs). This yields the following linear matrix representation of a broader class of energy hubs:

$$\widehat{\mathbf{P}}_h[k] = \mathbf{F}_h^{PWL} \Delta \widehat{\mathbf{P}}_h[k] \qquad (24)$$
$$\mathbf{L}_h[k] = \mathbf{C}_h^{PWL} \Delta \widehat{\mathbf{P}}_h[k] + \mathbf{S}_h^{out} \mathbf{Q}_h^{out}[k] \qquad (25)$$
$$\mathbf{D}_{\Delta,h}^{PWL} \mathbf{y}_h[k] \leq \mathbf{D}_h^{PWL} \Delta \widehat{\mathbf{P}}_h[k] \qquad (26)$$
$$\mathbf{D}_{adj,h}^{PWL} \mathbf{y}_h[k] \leq 0 \qquad (27)$$
$$\mathbf{C}_h^{out} \Delta \widehat{\mathbf{P}}_h[k] \leq \overline{\mathbf{L}}_h \qquad (28)$$
$$\Delta \widehat{\mathbf{P}}_h[k] \in [0, \Delta_h] \qquad (29)$$

for every hub $h \in \mathcal{H}$. Again, no coupling exists between hubs, so block diagonal versions of matrices $(.)_h$ represent all of $\mathcal{H}$.

C. Energy Hub Emissions

The impact of underestimating the converter input leads to inaccurate representation of costs and hub converter dispatches as shown in the case study, however, it also underestimates the emissions. This is because emissions is a linear function of converter input (i.e., the dispatch flow, $\widehat{P}_{ij}$).

Denote the emission output (e.g., CO_2, NOx, or SOx) from dispatch flow ij by $\widehat{e}_{ij}$ and the rate at which input is converted to emissions by β_{ij} (e.g., kg/MJ). Then, the relationship between emissions and converter input is:

$$\widehat{e}_{ij}[k] = \beta_{ij} \widehat{P}_{ij}[k]. \qquad (30)$$

Thus, if you underestimate $\widehat{P}_{ij}$, you underestimate $\widehat{e}_{ij}$. In fact, at low part-load operations, emission control systems are often unable to satisfy emission standards.

With the PWL approximation of converter nonlinearities, the converter input and (fuel) cost calculation is more accurate, which improves not just dispatch of converters, but also captures emissions more accurately. This is a significant benefit of the PWL approximation.

Combining the emissions from all converters in a single hub (or a set of hubs), we can apply an emission limit over a single hour or collection of hours (e.g., a 24-hour day). For example,

$$e_h[k] = \sum_{i=1}^{N_{in}} \sum_{j=1}^{K_i} \widehat{e}_{ij}[k] = \sum_{i=1}^{N_{in}} \sum_{j=1}^{K_i} \beta_{ij}^h \widehat{P}_{ij}[k] = \leq \overline{e}_{h,k}, \quad (31)$$

which is implemented in this work and has matrix notation:

$$\mathbf{F}_{\beta,h}^e \widehat{\mathbf{P}}_h[k] \leq \overline{\mathbf{e}}_h \quad (32)$$

Remark 3. In the energy hub literature, emissions are often included only in the objective function with a pre-defined carbon-tax (e.g., \$/kgCO2); however, in this work, emissions are included as constraints to allow insight into the marginal cost of emissions when constraints are binding. This is useful information for city-planners and policy makers who are trying to ascertain the "value" of CO2 under various emission policy scenarios.

D. Network of energy hubs

Energy hubs are interconnected either directly (as in this paper) or via adjacent energy supply networks. To describe the flow of energy *between* hubs, it is generally necessary to include power networks. A power network is a simple graph with sinks (e.g., loads) and sources (e.g., generators) and additional physical constraints corresponding to the specific nature of the network, e.g. balanced or unbalanced AC electrical system or natural gas pipelines. *Every network must satisfy flow balance.* That is, the sum of flows into and out of node i must equal the flow injected or consumed at node i. Additionally, with the inclusion of energy hubs, there is a need to consider flows between energy hubs and networks at each node. Thus, the flow balance equation can be generalized to that of an interconnected system of energy hubs:

$$A\mathbf{f} + H_I \mathbf{P} + H_O \mathbf{L} + G_A \mathbf{f}_G + D_A \mathbf{f}_D = \mathbf{0} \quad (33)$$

where $\mathbf{f}$ is the vector of directed network line flows, $\mathbf{P}$ is the vector of all hub inputs, $\mathbf{L}$ is the vector of all hub outputs, $\mathbf{f}_G$ is the vector of all generator injections, $\mathbf{f}_D$ is the vector of all consumer energy demands, A is the node-arc incidence matrix, H_I is the hub input incidence matrix, H_O is the hub output incidence matrix, G_A is the generator-node incidence matrix, and D_A is the load-node incidence matrix. For example, if hub input P_l is connected to node i then $H_I(i,l) = 1$, and if generator f_{G_k} is at node i then $G_A(i,k) = -1$. Otherwise the entries are all zeros. The other two matrices are defined in a similar manner. Since no control over the network topology is assumed, the matrices are constant parameters. Thus, we can restate (33) in terms of function Λ_n for network n,

$$\Lambda_n(\mathbf{f}, \mathbf{f}_G, \mathbf{f}_D, \mathbf{P}, \mathbf{L}) = \mathbf{0}. \quad (34)$$

As shown in (34), the connection between energy hubs and power networks only exists at hub inputs and outputs. In addition, energy hubs provide the opportunity for coupling multiple energy networks.

E. Multi-Period Optimal Dispatch Formulation

Combining the PWL linear energy hub and network models discussed in the previous sections, together with an objective function one can form an appropriate optimization problem. The optimization problem considers a prediction-horizon of T time-steps, $k = \{0, 1, \ldots, T-1\}$. The objective function maps systems states and control variables to a scalar cost and the goal of optimization is to reduce the cost of operating the multi-energy system (i.e. provide energy to satisfy demands at lowest cost possible). This is similar to the economic dispatch problem in electric power systems and, thus, the multi-energy optimization problem is denoted the **Multi-Period Optimal Dispatch** (MPOD) problem

$$\min_{\widehat{\mathbf{P}}, \mathbf{f}_G, \mathbf{Q}} \quad \sum_{k=0}^{T} \mathcal{F}\left(\mathbf{P}[k], \mathbf{L}[k], \mathbf{E}[k], \mathbf{f}_D[k], \mathbf{f}_G[k]\right) \quad (35)$$

subject to

$$(8) - (12), (24) - (29), (32), \text{ and } (34) \; \forall h, n, k$$
$$\text{and bounds on all variables}$$

Solving the MPOD problem is equivalent to solving a multi-period mixed-integer quadratic (mathematical) program (MIQP), which is NP-hard in general. However, state-of-the-art solvers can efficiently find near-optimal feasible solutions. Below, we leverage GUROBI 6.5.0 on a personal laptop computer to solver the MPOD problems.

III. Automated Analysis: Hubert

In [12], we introduced Hubert, which is a flexible tool that leverages a concise ASCII energy hub description format and interfaces with MATLAB and optimization solvers. In our prior work, Hubert did not consider nonlinear or output-constrained converters nor hub emission constraints (because the focus was on large-scale multi-carrier networks and not the dispatch of energy hub converters). However, in the study of city-scale multi-energy systems, nonlinear conversion processes are important to consider. Thus, this paper improves Hubert by enabling the modeling of nonlinear output-constrained hub converters and hub emission limits. The nonlinearity is represented by a set of $S + 1$ salient converter input-output pairs and Hubert takes care of forming the proper matrices, constraints, and variables for solving the resulting MPOD problem. Figure 4 illustrates the updated "Hub" description, which is described in detail in [12].

IV. Case-study: Multi-Energy University Campus

To illustrate the PWL energy hub formulation, we apply the updated Hubert to University of Vermont's (UVM's) heating/cooling/electric system, which can be represented as a network of two interconnected energy hubs. UVM's energy plant currently consists of five large steam boilers (gas in; heat out), two steam-driven compression chillers (heat in; cooling out), a distribution-level transformer (electric in and out) and heating, cooling and electric loads as shown in Fig. 5a. Local gas and electric utilities supply the necessary input sources (e.g., a $\approx$12MW electric peak).
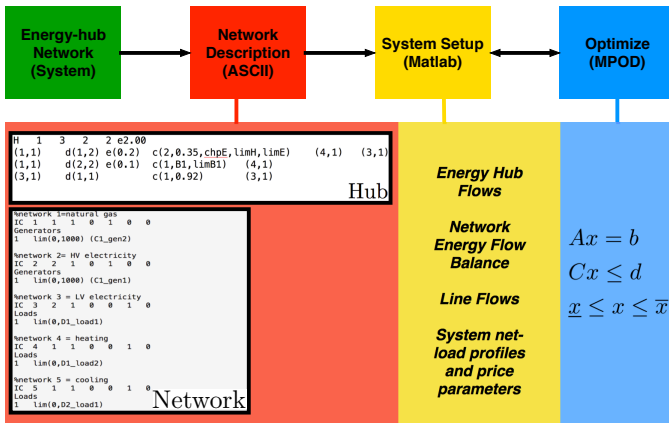
Converter	B_1	B_5	C_1^S	C_3^E	CHP(e)
Output limit (pu)	1.142	1.782	0.492	0.528	0.55
Constant eff (%)	80.0	80.5	145	900	38.0

TABLE I: Per-unit converter output limits. Note that chiller efficiency greater than 100% is intended due to COP> 1.

Figure 4: Overview of Hubert data flow. The updated Hubert format in "Hub" allows for emission limits (`e2.00`), emission factors (`e(0.2)`, `e(0.1)` in per-unit), PWL converters (`chpE` and `B1` are $(S+1) \times 2$ matrixes with $S+1$ I/O pairs) and converter output limits (scalars: `limH`, `limE`, `limB1`). Note that the alpha-numeric variable names are described in a MATLAB structure as detailed in [12].
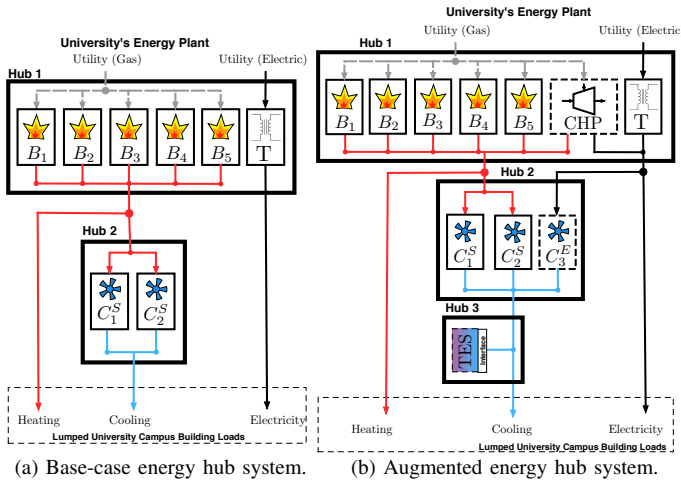

(a) Base-case energy hub system.   (b) Augmented energy hub system.

Figure 5: Modeling UVM energy system with energy hubs.

With system base values chosen as: 1pu=10MW; 1eu=MWh; 1mu=\$10,000, the utilities' daily rates can be represented with constant hourly natural gas prices (0.1727 mu/pu) and time-of-use electric rates (0.7919-1.1546 mu/pu) that include the effect of electrical demand charges. First, we illustrate the impact of nonlinear and linear converter models for a winter (heating) load scenario with the system from Fig. 5a. Second, we will augment the system with cogeneration (CHP), an electric chiller, and thermal energy storage (TES) to better understand scalability of Hubert and impact on savings – see Fig. 5b.

A. Hubert Simulations

For each of the nonlinear converters, we utilize a 10-segment equispaced PWL approximation, which is excessive but provides a measure of scale in the number of binary variables. The per-unit input-output curve of each converter is given by:

B_1:   out $= -0.357\mathrm{in}^3 + 0.890\mathrm{in}^2 + 0.267\mathrm{in}$

B_5:   out $= -0.155\mathrm{in}^3 + 0.587\mathrm{in}^2 + 0.267\mathrm{in}$

C_1^S: out $= 139.07\mathrm{in}^4 - 100.78\mathrm{in}^3 + 19.518\mathrm{in}^2 + 0.779\mathrm{in}$

C_3^E: out $= -3952.77\mathrm{in}^3 + 400.05\mathrm{in}^2 - 1.017\mathrm{in}$

chp-e: out $= 0.1629\mathrm{in}^2 + 0.08\mathrm{in}$

chp-h: out $= 0.40\mathrm{in}$

T: out $= 0.92\mathrm{in}$

Boilers 2, 3, and 4 are identical to B_1, except for a reduction in efficiency of 2%, 4%, and 5%, respectively. Steam-driven chiller 2 is identical to C_1^S, except for a 5% reduction in efficiency. The per-unit converter output limits are given by Table I. The chilled-water TES has power/energy rating 0.50 pu / 4.0 eu and charge/discharge efficiency of 99%/95%.

1) Comparing Constant vs. Variable Efficiency: From the input-output curves, the efficiency at rated output is chosen as value in the constant-efficiency energy hub comparison study and are provided in Table I. The base-case system in Fig. 5a is then simulated in Hubert under constant and variable efficiency assumptions. The boiler dispatch is shown in Fig. 6. Unlike with constant efficiency converters, nonlinear converters create a natural incentive to operate near optimum efficiency, which discourages low part-load operation. This is particularly clear in hours 4 and 14-18 where the boilers are dispatched very differently. In fact, the 24-hour natural gas cost of the constant efficiency dispatch is 2% higher (+\$3,740) than the dispatch with the nonlinear converters due to part-load operation. These savings can be significant during a long winter. The PWL formulation of the base system has 3048/2640 binary/continuous variables, 7270 constraints, and solves to optimality in less than one second.

2) Comparing Augmented Systems: The augmented system is now simulated in Hubert. As expected, low natural gas prices and high electric rates make the CHP a wise investment that drives down total energy costs by 30% (-\$132,000) In fact, the addition of the chiller and chilled-water TES decreases costs by less than 1% in each case, but offers other operational improvements (e.g., reliability through redundancy). Again, the augmented systems' constant-efficiency converter case leads to a total dispatch cost that is $\approx 3\%$ higher (+\$10,000) than the PWL converters. Interestingly, the two augmented cases dispatch storage very differently, as shown in Fig. 7. The PWL converter utilizes the highly efficient TES as a buffer to keep converters near maximum efficiency and charges/discharges the TES to make up the difference with the cooling loads while the constant-efficiency case leverages (fictitiously) efficient part-load operation. For example, had the constant-efficiency hub system study been used for sizing the TES, the TES would have been sized too
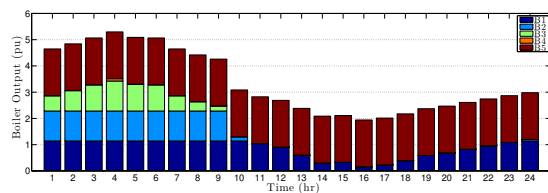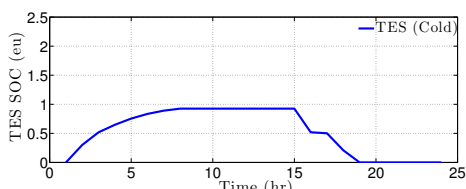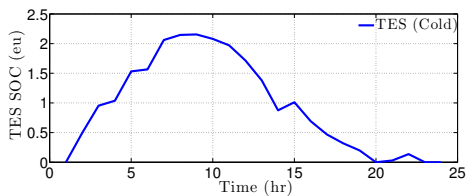
(a) Constant efficiency.
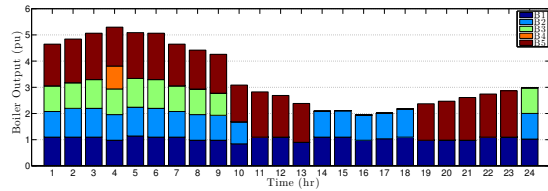
(b) Variable efficiency

Figure 6: Base-case optimal boiler dispatch.

(a) Constant efficiency.

(b) Variable efficiency

Figure 7: Optimal TES dispatch for augmented systems.

small. This further illustrates the benefit of PWL formulation. The PWL formulation of the augmented system has 3984/3504 binary/continuous variables, 9598 constraints, and solves to within a 0.15% optimality gap in 30 seconds.

V. CONCLUSION AND EXTENSIONS

This paper presents a computationally efficient model for a broad class of energy hub systems that can be effectively optimized with the simple description. Specifically, it has been shown that a PWL energy hub formulation is tractable for a meaningful system and provides superior performance over the common constant energy converter models (w.r.t. costs and optimal dispatch). Furthermore, results highlight the significant reduction in effects inherit to constant efficiency energy hubs in supporting operational and capital planning decisions (e.g., converter sizing/siting problems). Hubert will be extended to include unbalanced distribution systems, which are important at the city-scale. With regards to converter models, we are currently in the process of configuring real-time data gathering capabilities at the UVM energy plant to improve converter

and emission models and seek to expand the hub system to include additional multi-energy generation, networks, and loads in support of operational and capital planning decision-making. Long-term, we are interesting in exploring effect of increased renewable penetration at city-level and effect of emission standards, electrified transportation, and reliability of supply in MES.

REFERENCES

[1] P. Mancarella, "MES (multi-energy systems): An overview of concepts and evaluation models," *Energy*, vol. 65, no. c, pp. 1–17, Feb. 2014.

[2] D. M. Marsh, "The Water-Energy Nexus: A Comprehensive Analysis in the Context Of New South Wales," Ph.D. dissertation, University of Technology, Sydney, 2008.

[3] T. Boston, "State of the PJM Community," in *PJM Annual Meeting*, PJM. Maryland: PJM, May 2014.

[4] M. Almassalkhi, B. Simon, and A. Gupta, "A novel online energy management solution for energy plants," in *IEEE Power Systems Conference*, Mar 2014.

[5] M. Geidl, G. Koeppel, P. Favre-Perod, B. Klockl, G. Andersson, and K. Fröhlich, "Energy hubs for the future," *IEEE Power and Energy Magazine*, vol. 5, no. 1, pp. 24–30, 2007.

[6] A. Hajimiragha, C. Canizares, M. Fowler, M. Geidl, and G. Andersson, "Optimal Energy Flow of integrated energy systems with hydrogen economy considerations," in *Bulk Power System Dynamics and Control - VII. Revitalizing Operational Reliability, 2007 iREP Symposium*. IEEE, 2007, pp. 1–11.

[7] M. Geidl and G. Andersson, "Optimal Coupling of Energy Infrastructures," *IEEE PowerTech*, pp. 1398–1403, 2007.

[8] T. Krause, G. Andersson, K. Fröhlich, and A. Vaccaro, "Multiple-Energy Carriers: Modeling of Production, Delivery, and Consumption," *Proceedings of the IEEE*, 2010.

[9] M. Arnold, R. Negenborn, G. Andersson, and B. D. Schutter, "Distributed Predictive Control for Energy Hub Coordination in Coupled Electricity and Gas Networks," *Intelligent Infrastructures*, pp. 235–273, Jan. 2010.

[10] E. Fabrizio, V. Corrado, and M. Filippi, "Renewable Energy," *Renewable Energy*, vol. 35, no. 3, pp. 644–655, Mar. 2010.

[11] M. Almassalkhi, "Optimization and Model-predictive Control for Overload Mitigation in Resilient Power Systems." Ph.D. dissertation, University of Michigan, Ann Arbor, MI, May 2013.

[12] M. Almassalkhi and I. A. Hiskens, "Optimization Framework for the Analysis of Large-scale Networks of Energy Hubs," *Power Systems Computations Conference*, Aug. 2011.

[13] ——, "Impact of Energy Storage on Cascade Mitigation in Multi-energy Systems," *IEEE Power and Energy Society General Meeting*, Jul. 2012.

[14] M. C. Bozchalui, S. A. Hashmi, H. Hassen, C. A. Canizares, and K. Bhattacharya, "Optimal Operation of Residential Energy Hubs in Smart Grids," *IEEE Transactions on Smart Grid*, vol. 3, no. 4, pp. 1755–1766, 2012.

[15] X. Zhang, M. Shahidehpour, A. Alabdulwahab, and A. Abusorrah, "Optimal Expansion Planning of Energy Hub With Multiple Energy Infrastructures," *IEEE Transactions on Smart Grid*, vol. 6, no. 5, pp. 2302–2311, Sep. 2015.

[16] S. Bahrami and A. Sheikhi, "From Demand Response in Smart Grid Toward Integrated Demand Response in Smart Energy Hub," *IEEE Transactions on Smart Grid*, vol. PP, no. 99, pp. 1–1, 2015.

[17] G. Beccuti, T. Demiray, M. Batic, N. Tomasevic, and S. Vranes, "Energy hub modelling and optimisation: an analytical case-study," in *PowerTech, 2015 IEEE Eindhoven*. IEEE, 2015, pp. 1–6.

[18] S. Le Blond, R. Li, F. Li, and Z. Wang, "Cost and emission savings from the deployment of variable electricity tariffs and advanced domestic energy hub storage management," in *PES General Meeting — Conference & Exposition, 2014 IEEE*. IEEE, 2014, pp. 1–5.

[19] S. Paudyal, C. A. Canizares, and K. Bhattacharya, "Optimal Operation of Industrial Energy Hubs in Smart Grids," *IEEE Transactions on Smart Grid*, pp. 1–20, Jan. 2014.

[20] E. Fabrizio, "Modelling of multi-energy systems in buildings," Ph.D. dissertation, Politecnico di Torino, Torino, Italy, Jul. 2008.

[21] M. Almassalkhi and I. A. Hiskens, "Cascade mitigation in energy hub networks," in *IEEE Conference on Decision and Control and European Control Conference*. Department of Electrical Engineering and Computer Science, Dec. 2011, pp. 2181–2188.